

# Mussel Disturbance Dynamics: Signatures of Oceanographic Forcing from Local Interactions

Frédéric Guichard,<sup>1,\*</sup> Patti M. Halpin,<sup>2,†</sup> Gary W. Allison,<sup>2,‡</sup> Jane Lubchenco,<sup>2</sup> and Bruce A. Menge<sup>2</sup>

1. Department of Ecology and Evolutionary Biology, Princeton University, Princeton, New Jersey 08544;

2. Department of Zoology, Oregon State University, Corvallis, Oregon 97331

*Submitted December 17, 2001; Accepted September 13, 2002;  
Electronically published June 10, 2003*

---

**ABSTRACT:** Local interactions, biotic and abiotic, can have a strong influence on the large-scale properties of ecosystems. However, ecological models often explore the influence of local biotic interactions where physical disturbance is included as a large-scale and imposed source of variability but is not allowed to interact with biotic processes at the local scale. In marine intertidal communities dominated by mussels, wave disturbances create gaps in the mussel bed that recover through a successional sequence. We present a lattice model of mussel disturbance dynamics that allows local interactions between wave disturbance and mussel recolonization, in which each cell of the lattice can be empty, occupied by a mussel bed element, or disturbed (which corresponds to a newly disturbed cell that has unstable edges). As in natural ecosystems, wave disturbance can also spread from disturbed to adjacent occupied cells, and recolonization can also spread from occupied to adjacent empty cells. We first validate the local rules from artificial gap experiments and from natural gap monitoring along the Oregon coast. We analyze the properties of the model system as a function of different oceanographic forcings of productivity and disturbance. We show that the mussel bed can go through phase transitions characterized by a large sensitivity of mussel cover and patterns to oceanographic forcings but also that criticality (scale invariance) is observed over wide ranges of parameters, which suggests self-organization. We also show that spatial patterns in the intertidal can provide a robust signature of local processes and can inform about oceanographic regimes. We do so by comparing the large-scale patterns of the simulation (scaling ex-

ponents) with field data, which suggest that some experimental sites are close to criticality. Our results suggest that regional patterns in disturbed populations can be explained by local biotic and abiotic processes submitted to oceanographic forcing.

*Keywords:* wave disturbance, benthic communities, lattice model, self-organization, scale invariance, criticality.

---

Explaining the macroscopic properties of ecosystems from our understanding of local interactions is a great challenge for ecologists (Levin 1992; Milne 1998). One of the first steps toward this goal is to identify the minimum set of microscopic states and interactions within ecosystems that are required to explain large-scale patterns. Theoretical ecology has explored large-scale properties that emerge from systems where individuals and populations interact in space and time (Tilman and Kareiva 1997). Statistical mechanics is also increasingly applied to ecological systems (Kizaki and Katori 1999; Solé et al. 1999) and allows one to identify scale-invariant properties in model ecosystems. These theoretical efforts allow us to look for similarities between ecological and other simple physical systems. While models that are based on local interactions can be tested using small-scale experiments, they also make specific predictions about large-scale dynamics and patterns that can then be measured in the field. Most of these efforts have been built on the assumption that local interactions are dominated by biotic processes while environmental complexity constrains community dynamics at larger spatial scales (Bascompte and Solé 1995; Pacala and Levin 1997). Here, we present a model of wave-disturbed mussel beds. The model is similar to forest fire models (FFM; Drossel and Schwabl 1992; Clar et al. 1999) and models of epidemics (Rhodes et al. 1997). We include local interactions among elements of the mussel bed and between the mussel bed and wave disturbance so that both biotic and abiotic processes are fully described at the local level.

Theoretical models of intertidal systems have often treated biotic disturbance as a result of biotic interactions among species under large-scale environmental forcing (Possingham and Roughgarden 1990). This approach pre-

\* Corresponding author. Present address: Biology Department, McGill University, 1205 Avenue Doctor Penfield, Montreal, Quebec H3A 1B1, Canada; e-mail: frederic.guichard@mcgill.ca.

† Present address: Department of Biology, Arizona State University, Tempe, Arizona 85287.

‡ Present address: Department of Evolution, Ecology and Organismal Biology, Ohio State University, Columbus, Ohio 43210.

Am. Nat. 2003. Vol. 161, pp. 889–904. © 2003 by The University of Chicago. 0003-0147/2003/16106-0104\$15.00 All rights reserved.

cludes the possibility of environmental complexity interacting explicitly with biotic interactions at the local scale. Individual-based and spatially explicit models, because of their complexity, are limited to spatial extents that are much smaller than patterns and processes associated with wave disturbance (ones to hundreds of meters). The patch dynamics and patch mosaic approaches applied to disturbed systems (Dayton and Tegner 1984; Dayton et al. 1984) addressed this problem by simplifying space and individual behavior into homogeneous patches that correspond to disturbed areas (Levin and Paine 1974; Paine and Levin 1981; Reise 1991) in which local interactions are ignored.

An alternative approach that allows one explicitly to include the local interactions of gap formation and recovery without restricting the spatial extent of simulations is to aggregate individuals and species into community elements within a lattice model where space occupancy is defined in each cell of the lattice by a set of predefined community elements. A lattice-based approach to disturbed-systems modeling has been used to implement mussel bed dynamics (Wilson et al. 1996; Wootton 2001) and also simple predator-prey interactions (Tainaka 1989; Solé and Valls 1992), FFM (Drossel and Schwabl 1992; Clar et al. 1999; Malamud et al. 1998), and epidemics (Keeling 2000). In these latter models, cells can be empty, occupied by a susceptible individual (tree in FFM), or occupied by an infected individual (burning tree in FFM). Local interactions are then implemented as the spreading of infected individuals to their nearest neighbors.

Critical phenomena theory has contributed to the understanding of such simple lattice models and, more generally, to the understanding of spatial patterns in interacting particle systems submitted to external forcings. In these model systems, each particle is a site defined by its position and state on a lattice and interacts only with its neighbors according to predefined rules. Since forcing (control) parameters are varied across critical values, the macroscopic state of these systems (i.e., global state variables) goes through very sharp transitions, usually from an ordered phase where all sites share the same state to a disordered phase where states are randomly distributed across the lattice. At the transition point (i.e., when the control parameter is at the critical value), the system is said to be critical, meaning that many of its properties, such as the frequency distribution of clusters, are scale free or scale invariant (i.e., the cluster size distribution follows a power law function). One consequence of criticality is the emergence of long-range (large-scale) correlation over the lattice from local rules, since the scale-free distribution of cluster size implies that clusters of all sizes are present over the lattice. The scaling exponent, the exponent of these scale-invariant distributions, provides a quantitative

signature of the local rules that regulate the system and a means for comparing the behavior of different systems. For some systems, such as FFM, criticality has been shown to occur over a wide range of parameter values rather than requiring any fine tuning of parameters that characterize phase transitions (Malamud et al. 1998; Clar et al. 1999). This phenomenon has been referred to as self-organized criticality (SOC) and has been of interest in ecology to explain the observation of scale invariance in ecological systems (Solé and Manrubia 1995a, 1995b; Rohani et al. 1997; Kizaki and Katori 1999). We argue that this class of system can describe wave-disturbed mussel beds, and we more precisely explore the emergence of scale-invariant patterns in relation to oceanographic conditions.

Along the Oregon coast, midzone intertidal communities are dominated by the mussel *Mytilus californianus*. Mussels are disturbed by strong waves, mostly during winter, that create gaps in the mussel bed (Paine and Levin 1981; Menge and Sutherland 1987). These gaps are colonized by subdominant species that facilitate or precede recruitment by *M. californianus*. Because the number of successional species is high, which can complicate spatially explicit models, we view succession from gaps to mussel bed as the transition between discrete community elements or functional groups. The simplest functional grouping is to define space as being empty or occupied by a mussel bed (i.e., mussels and associated species). When a gap is created by wave action, edges of the gap consist of mussels that lost their byssal thread attachment to some of their neighbors and to the substratum. As a consequence, edges of a newly formed gap are temporarily unstable and more susceptible to disturbance than are other areas of the bed (Denny 1987). Local disturbance can then be implemented by defining disturbed areas as newly created gaps that have unstable edges from which wave disturbance can spread. Although mussels may recruit into both bare space and existing bed, the importance of conspecific density has been shown for mussel recruitment, survival, and growth (Svane and Setyobudiandi 1996; Helmuth 1998). Additionally, the lateral movement of adult mussels into bare space is the primary method of recolonization immediately following disturbance (Paine and Levin 1981). Therefore, in this article, we explore the dynamics of a model mussel bed system where disturbance and recovery are implemented as local processes.

First, we present our model and test its local rules by using experimental data. Then, we explore the behavior of the lattice model over gradients of disturbance and recovery rates. We show how local disturbance and recovery rules interact to produce patterns usually explained by large-scale environmental complexity. Furthermore, we look for signatures in spatial patterns that can be compared with empirical data in order to quantify the potential im-

portance of local endogenous processes for the formation of large-scale patterns in mussel beds. Finally, we derive the mean-field theory to assess the role of spatial interactions for mussel bed dynamics.

The Model

First, we describe a lattice model of mussel disturbance dynamics. Although the model is applied to a wave-disturbed intertidal system, disturbance is implemented as a generic epidemic and could be applied to biotic disturbance such as predation. The model divides a whole mussel bench into 1-m<sup>2</sup> cells and implements local interactions among community elements that occupy space.

Succession in Mussel Bed Communities

While *Mytilus californianus* is the dominant species and ultimately wins competition for primary space occupancy by forming beds (Paine 1966, 1984), wave disturbance creates empty areas (gaps) and initiates a succession of opportunistic species that occupy these gaps until mussels recover and recolonize the available primary space (Paine and Levin 1981). The model we present simplifies this process by describing a succession among three states: disturbed (state 0), empty (state 1), and occupied by mussels (state 2). The disturbed state denotes newly disturbed mussel beds with unstable edges (destroyed byssal threads) where the disturbance is more likely to spread to occupied neighbors. The disturbed state is the equivalent of burning trees in FFM or infectious individuals in susceptible-infective-recovered models. Specifically, it allows inclusion of the physical disturbance as a microscopic property. The occupied state is actually a community element that aggregates species and individuals that form a mussel bed. Transitions reflect disturbance and biological processes (fig. 1). Empty space can be colonized by mussels through recruitment, growth, and local movement from occupied neighbors. The transition from occupied to disturbed occurs when wave disturbance removes the mussels from the cell. That cell remains in the disturbed state until any mussels in neighboring cells have rebuilt their byssal threads or become disturbed themselves, at which time the disturbed cell stabilizes and transitions to empty (fig. 1). By using this definition of disturbed cells, we make sure that occupied cells can be disturbed only from their unstable edge.

Because we aggregate individuals into discrete functional groups, transition rules reflect aggregated processes. We assume that the mussel bed can colonize only empty cells that have occupied neighbors, but we also report results from simulations that allow global colonization. The model allows two mechanisms for disturbance: initial

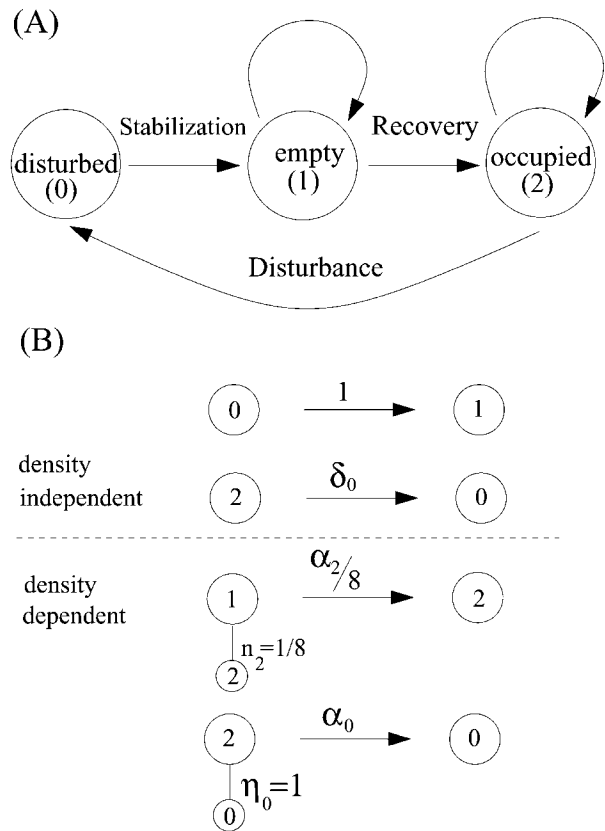


Figure 1: A, State transition diagram where each arrow shows a possible transition between two states in the model. B, Diagram of density-independent (top two transitions) and density-dependent (bottom two transitions) transition rates showing neighborhood effect. Transition probabilities are shown for transitions between different states (see text for symbol description). The third transition shown is from an empty site that has one occupied neighbor (local mussel cover  $n_2 = 1/8$ ; smaller circle) to an occupied cell. The last transition is from an occupied cell that has at least one disturbed cell ( $\eta_0 = 1$ ) to a disturbed cell.

disturbance and spreading. More precisely, wave disturbance can affect an occupied cell that has a disturbed cell in its neighborhood, but new disturbances can also dislodge mussels from occupied cells independently of neighborhood states. We assume that new disturbances affect only one cell in order to test the influence of disturbance spreading on gap size distribution, but we also report results from simulations that allow new disturbances to affect more than one cell.

Mussel Disturbance Dynamics

The dynamics in each cell can be described as a first-order nonlinear Markov chain with a transition matrix **W** that

defines transition probabilities applied to each cell over a lattice of size  $N^2$ . Empty cells are covered by a mussel bed with probability  $\alpha_2 n_2$ , where  $\alpha_2$  is the recovery probability and  $n_2$  is the proportion of occupied next-nearest neighbors (four nearest neighbors and four neighbors along diagonals). An occupied cell becomes disturbed with probability  $\alpha_0$  if at least one of its neighbors is disturbed (i.e., if  $n_0 \geq 0$ ; fig. 1).

Because they impose the overall rates of disturbance and recovery,  $\alpha_0$  and  $\alpha_2$  define the oceanographic forcings over the site. Thus, we assume that  $\alpha_2$  is a measure of productivity (sensu Menge et al. 1997a) at the site level and influences mussel recruitment and growth, and we assume that  $\alpha_0$  is a measure of wave exposure (i.e., force exerted on the bench by an average wave) over the site.

Density-independent transition probabilities include the probability  $\delta_0$  that an occupied cell becomes disturbed (initial disturbance) when a cell is updated and the stabilization of disturbed cells, which become empty with probability 1. This means that all other transition rates are normalized by the stabilization rate.

Thus, we compute each transition probability  $W(i, j)$  as the sum of local and global transition probabilities so that

$$\mathbf{W}(t) = \begin{bmatrix} 0 & 0 & \alpha_0 \eta_0 + \delta_0 \\ 1 & 1 - \alpha_2 n_2 & 0 \\ 0 & \alpha_2 n_2 & 1 - \alpha_0 \eta_0 - \delta_0 \end{bmatrix}. \quad (1)$$

Each entry  $W(i, j)$  of  $\mathbf{W}(t)$  specifies the transition probability in a single cell from the state in column  $j$  (corresponding to states 0, 1, 2) to the state in line  $i$ . The presence of at least one disturbed cell in the neighborhood is defined by  $\eta_0$ , with  $\eta_0 = 1$  if  $n_0 \geq 0$  and  $\eta_0 = 0$  if  $n_0 = 0$ .

The model was simulated on a two-dimensional lattice. We used periodic boundary conditions in order to avoid edge effect, with lattice size  $N = 512$ . The periodic boundary condition means that cells along an edge of the lattice will have neighbors along the opposite edge. The lattice was updated asynchronously in order to approximate a continuous-time process (Durrett and Levin 1994). During each simulation, cells were randomly selected for update during 4,000 time steps, with one time step equal to  $N^2$  individual cell updates. Analysis was carried out after removing the first 2,000 transient time steps. We also define  $\mathbf{C} = \{\rho_0, \rho_1, \rho_2\}$  as the cover vector of disturbed ( $\rho_0$ ), empty ( $\rho_1$ ), and occupied ( $\rho_2$ ) states on the lattice.

### Validating the Local Rules

#### *Artificial Gap Data*

We created experimental gaps in mussel beds at three sites along the Oregon coast (Strawberry Hill, Yachats Beach,

Boiler Bay/Fogarty Creek). We created two sets of gaps at each site in spatially separated beds; each set consisted of five gaps that were initially square and measured 1 m<sup>2</sup>. We created the gaps by manually removing all mussels and other organisms from the 1-m<sup>2</sup> area in early spring 1996. Reference bolts were attached in several spots inside the gap to facilitate spatially explicit analysis of recovery. Progression of gap recovery was documented by photography with several records taken per year through November 2000. Photographs were analyzed to record the cover of mussels and other organisms as well as bare rock. To produce transition data, we translated each point in this time series from percent cover estimates to one of two mutually exclusive states by the following rules: if a cell had  $\geq 50\%$  cover of adult mussels, it was considered occupied; otherwise, it was considered empty. The empty state typically consisted of bare space, barnacles, ephemeral algae, and/or juvenile mussels. These states were recorded for the original cell (1-m<sup>2</sup> gap) as well as for its neighbor cells.

We computed transition rates from empty (nonmussel cover) to occupied (mussel bed) as a function of mussel cover in the neighborhood ( $n_2$ ). For each artificial gap, we computed the ratio of the number  $N_{21}(n_2)$  of transitions from state 1 to state 2 with the proportion  $n_2$  of neighbors in state 2 over the number  $N_{*1}(n_2)$  of sites in state 1 with  $n_2$  in state 2. If we normalize by the overall proportion of 1  $\rightarrow$  2 transitions, we obtain

$$F_{21}(n_2) = \frac{N_{21}(n_2)N_{*1}^T}{N_{*1}(n_2)N_{21}^T}, \quad (2)$$

where  $N_{*1}^T$  and  $N_{21}^T$  are summed over all neighborhood configurations. The ratio between the 1  $\rightarrow$  2 transition rate with a  $n_2$  neighborhood and the overall 1  $\rightarrow$  2 transition rate is  $F_{21}(n_2)$ . Thus, it is a facilitation index of each  $n_2$  value for the 1  $\rightarrow$  2 transition, with values  $>1$  representing a positive influence of  $n_2$  on the transition rate. Results show that at the meter scale, the recovery rate between each sampling increased with the number of occupied neighbors (fig. 2A), from almost 1 with no occupied neighbors to more than four times higher than the mean transition rate with a fully occupied neighborhood.

We also used artificial gap data to determine the temporal scale of the model by computing each gap's recovery time. From 1996 to 2000, 63% of all gaps had recovered to mussel bed cover. Among artificial gaps that recovered, the average recovery time was 49 mo.

#### *Natural Gap Data*

To compare the model with the initiation and recovery of natural mussel gaps, we used a subset of data obtained from two sites on the Oregon coast that differed in both

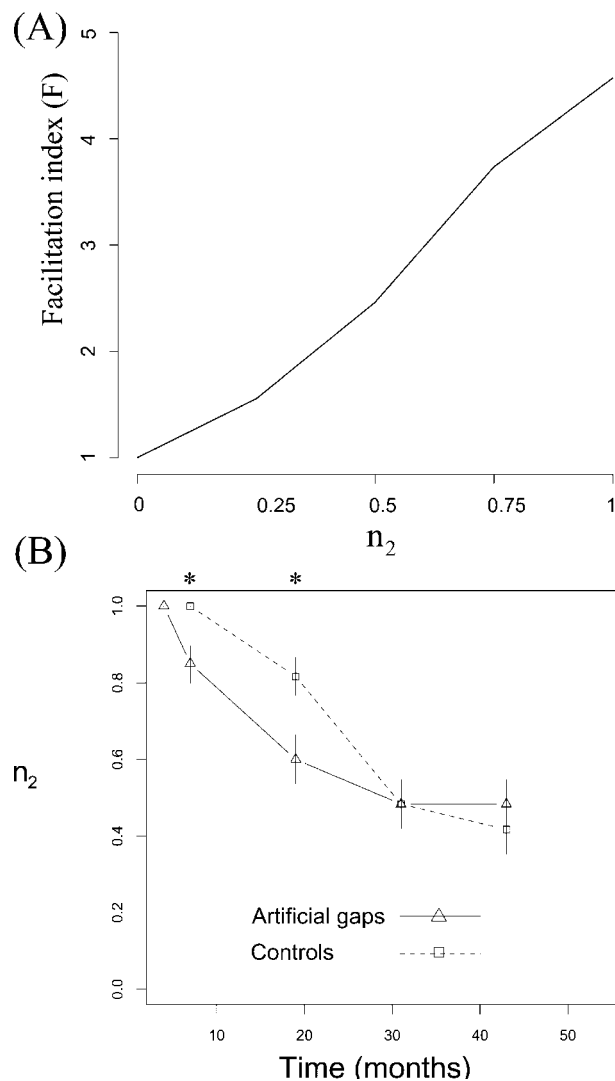


**Figure 2:** A, Influence of the neighborhood occupancy ( $n_2$ ) on recovery rate in the artificial gap experiment, from empty to mussel bed state. B, Proportion of occupied neighbors ( $n_2$ ) from 1996 to 1999, around experimental gaps (triangles) and control plots (squares) sampled from the natural gap data ( $\pm$  SE). Asterisks above data show sampling dates where significant differences between artificial gaps and controls were observed according to a MANOVA analysis ( $P < .01$ ).

growth rates of mussels and wave disturbance regime. The two sites, Boiler Bay/Fogarty Creek (44.84°N, 124.06°E) and Yachats (44.32°N, 124.12°E), are both broad, sloping benches with an unfragmented midintertidal zone dominated by *Mytilus californianus*. Mussel growth rates are higher at Yachats than they are at Boiler Bay/Fogarty Creek because of, in part, higher food content in the waters arriving onshore in the Yachats region (Menge et al. 1997a, 1997b). Within each site, two mussel beds were selected. From 1996 to 1999 at Boiler Bay/Fogarty Creek and from

1997 to 1999 at Yachats, the bed and mussel gaps were surveyed with a Topcon total station connected to an HP 256 calculator that ran TDS-48Gx software (Tripod Data Systems) to document spatial extent and orientation of gaps within the bed. Gaps were resurveyed every year in the summer to record disturbances from the previous winter and monitor recovery in previously surveyed gaps. Gaps that had no newly disturbed areas within them during the observation period were not surveyed every year. Because of frequent gap spreading, these unsurveyed gaps were a small proportion of the mussel bed area. Recovery was defined by the movement of edge mussels into previous gap area or when recruited *M. californianus* covered  $\geq 50\%$  of the gap area, at which point defining gap edges became impractical. Analysis was performed using ArcView 3.1 (ESRI) by converting survey data to polygons to distinguish gap and mussel bed areas. The polygon coverages were then converted to grids of cell size 1 m<sup>2</sup>. Transition rates were calculated by comparing grids between years.

For each year and at each mussel bed, we defined gap clusters as contiguous empty areas and mussel clusters as contiguous occupied areas. To examine the importance of local processes, we identified each disturbed or recovered cluster as being connected through its neighborhood or unconnected to a cluster of the same type from the previous year. This analysis was performed from the 1996 to the 1999 surveys. Assuming that recovered and disturbed areas were the result of spreading in the case of connected clusters and the result of nonlocal processes in the case of unconnected clusters, we can use this analysis to examine the relative importance of local processes (spreading) during disturbance and recovery at a temporal resolution of 1 yr.

On all beds, most of disturbed and recovered areas belonged to connected clusters (fig. 3). Recovery was mostly linked to existing bed clusters (96%–100% of recovered mussel beds; fig. 3B, 3D, 3F), which suggests that some recovery processes (recruitment, growth, predation refuges) involve local positive density dependence. Disturbances were also correlated with existing gaps, with connected disturbance being, in most cases, responsible for at least 80% of disturbances (fig. 3A, 3C, 3E).

Spreading of new disturbances can be examined by looking at mussel bed occupancy in the neighborhood of artificial gaps. Because these gaps are new disturbances at the beginning of the experiment, we used natural gap data to compare mussel cover in the neighborhood of artificial gaps with control areas where the mussel had not been experimentally disturbed. Control areas were selected by randomly sampling the GIS coverages of mussel bed. The analysis shows that the neighborhood of new disturbances is more likely to become empty than are control areas (fig.

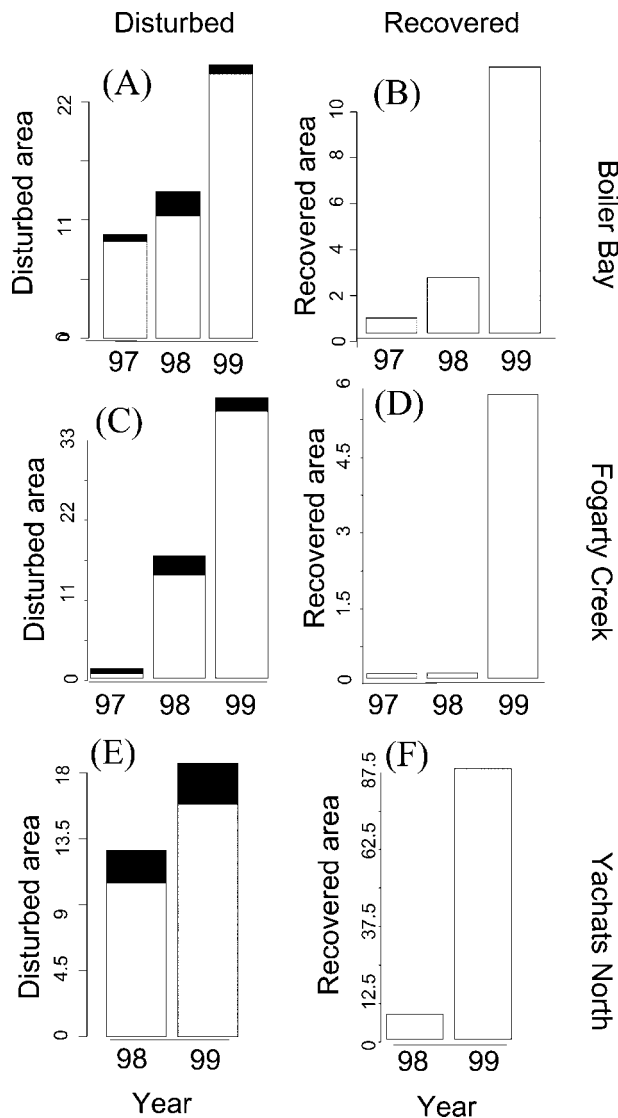


**Figure 3:** Disturbed (A, C, E) and recovered (B, D, F) areas shown as a percentage of total available area (mussel bed for disturbances and gaps for recolonization) and as connected (white) or unconnected (black) to clusters from the previous year. Data from Boiler Bay (A, B), Fogarty Creek (C, D), and Yachats North (E, F). Unconnected recovered areas on graphs are shown in B, D, and F but were too small to be visible in the figure.

2B; MANOVA repeated-measure analysis and Wilks's statistics,  $P < .01$ ), especially during the months following the disturbance (see the second observation in fig. 2B, 4 mo after artificial gaps were created). Artificial gaps were created during the spring, and they were the only areas around which wave disturbance was observed during the following summer (fig. 2B; P. M. Halpin, personal observation). While strong winter storms are responsible for most dis-

turbance events, weaker summer waves were able to spread only along edges of artificial gaps. This result is evidence that in the absence of strong waves (external disturbance), only recently disturbed unstable edges can be disturbed by average wave force. It also provides information about the temporal scale of the stabilization process ( $\approx 1$  mo).

Thus, results from artificial and natural gap experiments show that disturbance and recovery processes in intertidal mussel beds involve local correlation at the meter scale. More precisely, recently disturbed areas facilitate the disturbance of the neighboring mussel bed. The local processes involved in the spreading of wave disturbance have been discussed by Denny (1987), who suggests that lift forces that remove a few individuals could trigger the formation of larger gaps in the mussel bed. Paine and Levin (1981) assumed that gap size was fixed at birth or sampled after stabilization of disturbed areas. However, the high correlation between gaps and disturbance we observed suggests that the local processes might be important at a smaller temporal scale than the temporal scale of field observations. Recovery of a gap area is, in turn, facilitated by occupied neighbors. Positive density dependence during mussel bed recovery can be explained by observations that show that adult mussels move laterally along edges of gaps to occupy bare substratum (G. Allison, P. Halpin, J. Lubchenco, and B. Menge, unpublished results). Newly settled individuals also recruit near conspecifics (Bayne 1964) and find refuge against desiccation stress through aggregation (Helmuth 1998).

These results support the assumption that mussel disturbance dynamics can be defined at the local scale. We now turn to the model and examine the response of mussel cover (macroscopic property) to oceanographic gradients of productivity (recovery rate) and exposure (disturbance rate).

#### Incomplete Mussel Cover without New Disturbances

We can illustrate the behavior of the model across recovery and disturbance rates if we dynamically close the system by setting  $\delta_0 = 0$  so that no new disturbances can reach the bench. In that case, only the persistence of existing disturbances present as initial conditions can prevent mussels from completely covering the lattice. Although this is an unrealistic assumption about natural systems that will be relaxed in the next section, the simplification that results from it allows us to examine conditions for coexistence between disturbed and occupied sites by using a full mussel bed cover and one initial disturbance (one disturbed cell) as an initial condition. Using  $\alpha_0$  and  $\alpha_2$  as control parameters, we can define two conditions that lead to an absorbing state (complete mussel cover) where only occupied sites persist. First, when the disturbance rate is below the

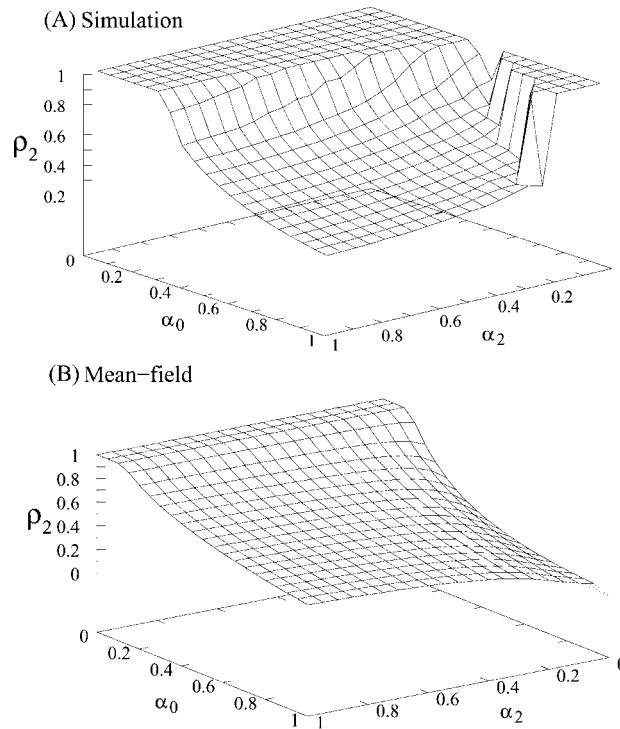


**Figure 4:** Mean mussel cover at equilibrium ( $\rho_2$ ) in the lattice simulation (A) and for the mean-field equations (B) as a function of recovery ( $\alpha_2$ ) and disturbance ( $\alpha_0$ ) rates.

critical value  $\alpha_0^* = 0.3$ , disturbed sites that form a disturbance front by spreading to neighbors and leaving behind empty sites are actually unable to spread successfully through the mussel bed. Second, for  $\alpha_0$  large and  $\alpha_2$  below the critical value  $\alpha_2^* \approx 0.25$  (for  $\alpha_0 = 1$ ), we observe an absorbing state (fig. 4A) that results from mussel density being low, right behind the disturbance front. As a result, the initial disturbance is able to spread through the initial mussel bed cover but is not in contact with the recovering mussels that will then cover the whole lattice without being disturbed unless the lattice is hit by a new wave disturbance. In other words, because disturbance is, in this case, much faster than recovery, the disturbance front is always ahead and, thus, never in close enough contact with recovering mussels. As a consequence, the disturbance is not able to spread back into the recovering bed and becomes extinct after having removed the initial bed. Thus, this absorbing state results from a separation of temporal scales between disturbance and recovery. When the disturbance is able to persist, mussel cover shows weak oscillations around a mean value, as shown in figure 4A. These mean values are quasi equilibria (sensu Day and Possingham 1995) since stochastic fluctuations in a finite-size system will eventually drive mussels to extinction in the absence

of global colonization. However, because of density-dependent local disturbance and the large lattice size, we were not able to observe mussel extinctions in simulations.

It is also possible to show that the critical value  $\alpha_2^*$  depends on initial conditions and, thus, is associated with hysteresis (fig. 5A). When we start the simulation with  $\alpha_2 > \alpha_2^*$  and progressively decrease  $\alpha_2$  below the critical value, each time after reaching equilibrium (after 2,000 time steps), the absorbing state is obtained for  $\alpha_2 < \alpha_2^* \approx 0.075$  (fig. 5A).

#### Phase Transitions in an Open System

These different regimes can be characterized as phase transitions defined as a rapid change in some system's property

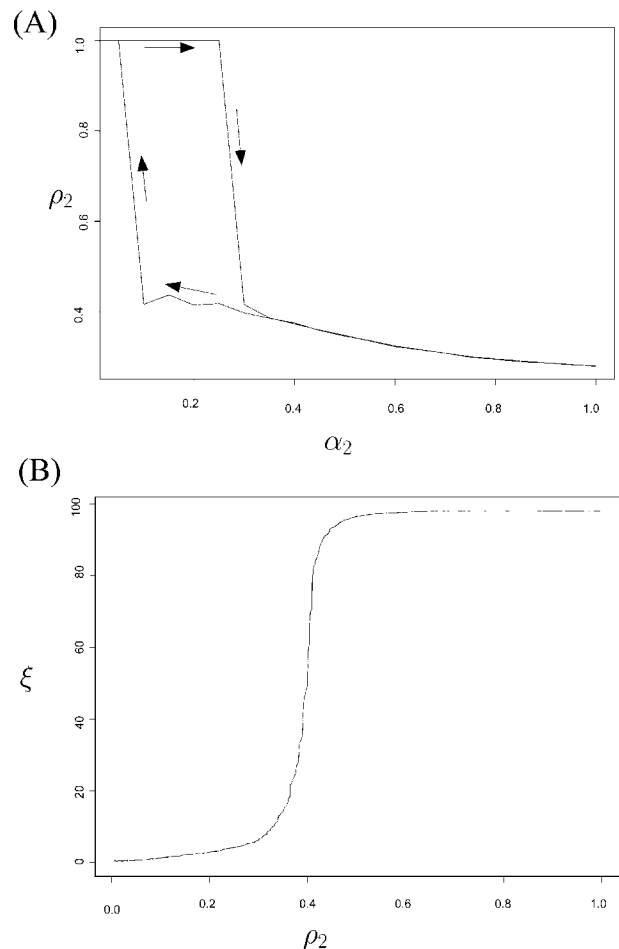


**Figure 5:** A, Mussel cover ( $\rho_2$ ) as a function of increasing and decreasing recovery rate ( $\alpha_2$ ). The arrows illustrate the hysteresis by showing that starting from  $\rho_2 = 1$  and progressively increasing  $\alpha_2$ , a transition occurs at  $\alpha_2 = 0.25$ . If we then progressively decrease  $\alpha_2$  to its original value, the transition will not take place until we reach  $\alpha_2 = 0.075$ . B, Correlation length ( $\xi$ ) as a function of mussel cover  $\rho_2$  for a passive percolation process.

(order parameter) when an external forcing (control parameter) is gradually varied across a critical value. When applied to mussel disturbance dynamics in which we allow new disturbances to reach the system ( $\delta_0 > 0$ ), we now show that the analysis of phase transitions provides a signature of oceanographic forcing defined by  $\alpha_0$  and  $\alpha_2$ . We can identify a phase transition from a near absorbing state ( $\rho_2 \rightarrow 1$ ) to the coexistence phase at the critical disturbance rate  $\alpha_0^*$  and for  $\alpha_2 > 0$ . No transition occurs at the critical recovery rate  $\alpha_2^*$  (fig. 4A) since the separation of temporal scales between disturbance and recovery for  $\alpha_2 < \alpha_2^*$  is now broken by new disturbances (table 1). As  $\alpha_0$  increases above  $\alpha_0^*$ , gaps not only persist but also quickly increase their ability to expand, as suggested by the fast decrease in mussel cover above  $\alpha_0^*$  (table 1). This decrease in  $\rho_2$  quickly reaches a threshold value  $\rho_2^* \approx 0.4$ , and the infinite mussel bed cluster (i.e., spanning across the whole lattice) is broken into finite size clusters (table 1). Thus, we can

define a clustering phase for  $\rho_2 < \rho_2^* \approx 0.4$  characterized by the coexistence of empty and occupied clusters and by the absence of an infinite mussel bed cluster.

Interestingly, the value of  $\rho_2^*$  corresponds to the next-nearest-neighbor percolation threshold (i.e., for  $q = 8$  neighbors). Percolation theory provides a framework to understand the spatial pattern and scaling properties of lattice models (Stauffer and Aharony 1992). It can be best understood by considering a lattice where sites can be either occupied or empty and by defining clusters as any set of occupied sites connected to each other through their neighbors. As the proportion  $p$  of occupied sites increases, larger clusters progressively form, and at some threshold value  $p_c$  (percolation threshold), one big cluster allows one to go from one side of the lattice to the opposite side by moving only on occupied sites (e.g., on the infinite mussel bed). This phenomenon can be quantified by the correlation length  $\xi$ , the average radius of mussel clusters on

**Table 1:** Scaling exponent  $\beta$  of the cluster size distribution and mean mussel cover  $\rho_2$  as a function of disturbance ( $\alpha_0$ ) and recovery ( $\alpha_2$ ) rates

$\alpha_2/\alpha_0$	.1	.2	.3	.4	.5	.6	.7	.8	.9	1
.1:										
$\beta$	...	...	...	...	...	...	...	...	...	1.94
$\rho$	1	1	1	.99	.81 (.02)	.65 (.04)	.56 (.04)	.50 (.04)	.46 (.05)	.41 (.04)
.2:										
$\beta$	...	...	...	...	...	...	...	...	...	1.99
$\rho$	1	1	1	.99	.75 (.01)	.62 (.02)	.54 (.02)	.49 (.02)	.45 (.02)	.42 (.03)
.3:										
$\beta$	...	...	...	...	...	...	...	...	2.02	1.99
$\rho$	1	1	1	.97	.70 (.01)	.58 (.01)	.51 (.01)	.46 (.02)	.43 (.02)	.40 (.02)
.4:										
$\beta$	...	...	...	...	...	...	...	1.94	1.93	1.91
$\rho$	1	1	1	.88	.65 (.01)	.54 (.01)	.48 (.01)	.43 (.01)	.40 (.01)	.38 (.01)
.5:										
$\beta$	...	...	...	...	...	...	...	1.83	1.81	1.82
$\rho$	1	1	1	.81	.62 (.01)	.52 (.01)	.45 (.01)	.40 (.01)	.37 (.01)	.35 (.01)
.6:										
$\beta$	...	...	...	...	...	...	...	1.75	1.74	1.75
$\rho$	1	1	1	.76	.59	.50 (.01)	.43 (.01)	.38 (.01)	.35 (.01)	.32 (.01)
.7:										
$\beta$	...	...	...	...	...	...	1.77	1.69	1.69	1.7
$\rho$	1	1	1	.73	.58	.48	.42	.37 (.01)	.33 (.01)	.31 (.01)
.8:										
$\beta$	...	...	...	...	...	...	1.72	1.65	1.65	1.68
$\rho$	1	1	1	.71	.56	.47	.41	.36	.32 (.01)	.30 (.01)
.9:										
$\beta$	...	...	...	...	...	...	1.7	1.62	1.64	1.67
$\rho$	1	1	1	.70	.56	.47	.40	.35	.32	.29
1:										
$\beta$	...	...	...	...	...	...	1.68	1.61	1.62	1.67
$\rho$	1	1	1	.69	.55	.46	.40	.35	.31	.28

Note: Ellipses show parameter values where an infinite cluster was observed in the cluster size distribution. We obtained  $\rho_2$  as the average cover over the last 2,000 time steps ( $SD \geq 0.01$  shown in parentheses). Variability in mean mussel cover among independent runs was undetectable ( $SE < 0.01$ ).



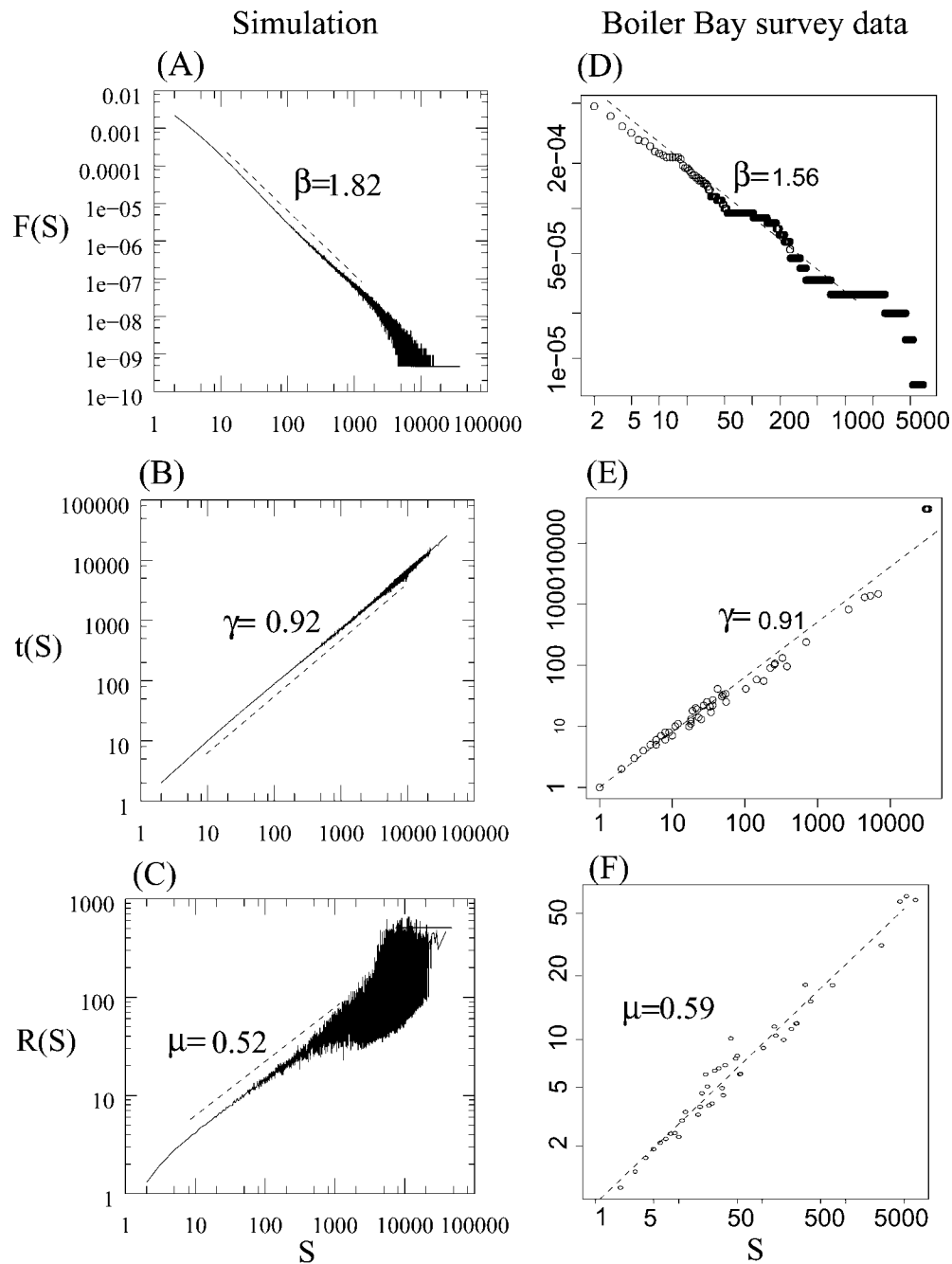


**Figure 6:** Frequency  $F(s)$  (A, D), interior area  $t(s)$  (B, E), and radius of gyration  $R(s)$  (C, F) of mussel bed clusters as a function of cluster size  $s$ , in the simulation for  $\alpha_0 = 1$  and  $\alpha_2 = 0.5$  (A–C) and from natural gap survey at Boiler Bay (D–F). Scaling exponents (slopes from linear regression performed on log transformed data) is shown for cluster size ( $\beta$ ), interior area ( $\gamma$ ), and the radius of gyration ( $\mu$ ).

the lattice (Binney et al. 1992), which increases with  $p$  and diverges at the percolation threshold  $p_c$  (fig. 5B). The percolation threshold is  $p_c = 0.5928$  for nearest-neighbor percolation ( $q = 4$  neighbors around each site). For next-

nearest-neighbor percolation ( $q = 8$ ), the percolation threshold is  $1 - p_c = 0.4072$  (Stauffer and Aharony 1992). This value is very close to the critical mussel density  $\rho_2^*$ , which suggests that the critical value defining the clustering

phase in the mussel disturbance model (MDM) involving local interactions is derived from a passive percolation process obtained without local density dependence for mussel colonization. We now look into more detail at the large-scale properties of the lattice within the clustering phase.

### Scaling Properties

The study of critical phenomena predicts that clusters have a scale-invariant size distribution near critical values (Binney et al. 1992). In other words, if we look at mussel clusters when the forcing parameters are at their critical value, the number of clusters  $F(s)$  of a given size  $s$  should decrease with  $s$  according to a power law so that  $F(s) \propto s^{-\beta}$ , where  $\beta$  is the scaling exponent (Binney et al. 1992). The power law characterizes scale invariance because the ratio of small to large cluster frequencies (slope of the power law function) is independent from the observation scale. In the MDM, we should expect criticality when  $\alpha_0$  and  $\alpha_2$  are at their critical value. This scaling is expected to vanish when the system moves away from the critical value, because cluster frequency decays faster than predicted by the power law distribution that characterizes scale invariance. The MDM has a well-defined clustering phase within the parameter space, where all three types (disturbed, empty, occupied) coexist and where the occupied state does not form an infinite cluster that spans across the lattice. The latter condition means that at equilibrium, the mean mussel cover is below the percolation threshold  $\rho_2^*$ . Within this clustering phase, mean mussel cover is weakly influenced by  $\alpha_2$  and  $\alpha_0$  with  $0.28 < \rho_2 < 0.4$  (table 1) and is increasing rapidly toward the absorbing state  $\rho_2 = 1$  close to  $\alpha_0^*$  (fig. 4A). Within the clustering phase, spatial patterns also have properties that are almost independent from parameter values. More precisely, we observe scale invariance in mussel beds as shown by the power law distribution  $F(s)$  of cluster size  $s$  (fig. 6A) with  $F(s) \propto s^{-\beta}$ , where  $1.61 \leq \beta \leq 1.99$ . The shape of mussel clusters is also characteristic within the coexistence region. We can first note that the perimeter of clusters (area in contact with other states) increases almost as fast as does cluster size (fig. 6B), which means that the amount of interface per cell is conserved as cluster size increases. The relationship between cluster perimeter and area actually follows a power law with scaling exponent  $\gamma = 0.92$ . When  $\gamma$  is close to 1, the amount of edges between mussel clusters and gaps is maximum, compared with an expected value of 0.5 for very compact clusters. As predicted for systems at criticality, clusters can also be shown to be fractal with dimension  $D = 1/\mu < 2$ , where  $\mu$  is the scaling exponent of the radius of gyration  $R(s)$  (average radius of a cluster; see Binney et al. 1992) as a function of cluster

size  $s$  (fig. 6C). This scaling is observed as long as  $\rho_2 < 0.4$  and does not vanish as control parameters ( $\alpha_0$  and  $\alpha_2$ ) are increased above their critical values.

We also tested the robustness of these results to the presence of global colonization  $\delta_2$ —that is, of empty  $\rightarrow$  mussel transitions that are independent from local mussel density—and to larger new disturbances. We repeated simulations with  $\delta_2 = 10\delta_0$  and with randomly selected new disturbance size ranging from 1 to  $0.01 \times N^2$  cells. The maximum size for new disturbances was set above the maximum relative disturbance size observed in natural gap data. For  $\alpha_0 > \alpha_0^*$ , results from this set of simulations ( $\rho_2$  and scaling exponents) were indistinguishable (difference  $< 10^{-2}$ ) from the reported results.

### Large-Scale Patterns in Natural Mussel Beds

We now look for these signatures in field data. Using the natural gap survey data, we can characterize spatial patterns in each of the three natural mussel beds. The model predicts that a mean mussel cover below  $\rho_2^*$  is in a critical state. This means that such a system should have long-range correlation that can be detected by power law scaling of the cluster size distribution and by the fractal shape of mussel clusters with  $D < 2$ . In one of the study sites, Boiler Bay, mussel cover declined from 0.8 in 1996 to 0.47 in 1999 (table 2). On this bench, we observe scale invariance in cluster size distribution with  $\beta = 1.56$  (fig. 6D) and fractal clusters with  $D = 1/\mu = 1.89$  (fig. 6F). Similar to simulation results, the area of cluster perimeter (the portion of a mussel bed cluster that is connected to a gap) also follows a power law distribution with scaling exponent  $\gamma = 0.91$  (fig. 6E), which is close to 1, the value expected if all sites within a cluster were part of the perimeter.

At Fogarty Creek, where mussel cover was higher than at Boiler Bay but decreased to values close to  $\rho_2^*$  (table 2), a scaling could be observed for  $\beta$ ,  $\gamma$ , and  $\mu$  (table 2). The scaling exponents measured at Fogarty Creek were similar to those measured at Boiler Bay, but scale-invariant patterns were valid up to a maximum cluster size of 12.5 m<sup>2</sup>, which defined the maximum size of mussel clusters. The mussel bed at Fogarty Creek was, thus, in a subcritical state where scale-invariant patterns are constrained by a maximum cluster size. This maximum cluster size was not observed in Boiler Bay where the break in the power law distribution (fig. 6D) is caused by a finite-size effect (cluster size is simply limited by habitat size).

For parameter combinations that lead to mussel cover above the critical value for clustering ( $\rho_2 > 0.4$ ), the model predicts the existence of an infinite cluster, with small gaps having a characteristic scale (no power law relationship in cluster size distribution). These small gaps are not able to expand their size and can persist by the balance between

recovery and disturbance spreading of each gap. These properties are observed at Yachats Beach, where mussel cover was always above 0.8, and where mussel clusters had a characteristic scale of 3.13 m<sup>2</sup>, which corresponds to the characteristic size of clusters within gaps.

### Mean-Field Theory

We now explore the behavior of the model under the simplifying assumption of well-mixed dynamics, which means that cells can interact with any other cell on the lattice. In the simulation, this assumption would require that neighbors are not limited to the eight nearest-neighbor cells but that they be selected at random from the whole set of sites. If we assume such a well-mixed community, we can use the cover vector  $\mathbf{C} = \{\rho_0, \rho_1, \rho_2\}$  of each state over the lattice instead of following the state of each cell.

The mean-field (MF) dynamics assumes that each cell interacts equally with all other cells on the lattice so that  $P(n_i = 1) = \rho_i$ , which means that  $n_i = \rho_i$  and  $P(n_i \geq 0) = 1 - (1 - \rho_i)^8$ . These approximations allow space to be included implicitly in the MF dynamics.

In continuous time, we obtain the following set of ordinary differential equations:

$$\begin{aligned} \frac{d\rho_0}{dt} &= \alpha_0 \rho_2 \{\delta_0 + [1 - (1 - \rho_0)^8]\} - \rho_0, \\ \frac{d\rho_2}{dt} &= \rho_2 (\alpha_2 (1 - \rho_0 - \rho_2) - \alpha_0 \{\delta_0 + [1 - (1 - \rho_0)^8]\}), \\ \rho_0 + \rho_1 + \rho_2 &= 1. \end{aligned} \quad (3)$$

We can show numerically that system 3 has a single, locally stable equilibrium for all values of  $\alpha_0$  and  $\alpha_2$  in the interval 0–1. For  $\delta_0 = 0$ , the stable equilibrium is the absorbing state  $\rho_2 = 1$  when  $\alpha_0 \leq \alpha_0^* = 0.125$ , and we observe a spiral sink equilibrium (i.e., decaying oscillations) for  $\alpha_2/\alpha_0 + 0.125 > 0.6$  (fig. 7A). It is also possible to show that  $\alpha_0^* = 0.125$  by noting that, at equilibrium,

$$\rho_2 = \frac{\rho_0}{\alpha_0 [1 - (1 - \rho_0)^8]} \quad (4)$$

and

$$\rho_0 = \frac{\alpha_2 \rho_2 (1 - \rho_2)}{1 + \alpha_2 \rho_2}. \quad (5)$$

These two functions intersect at the internal equilibrium (coexistence) as long as

$$\alpha_0 > \text{Lim}_{\rho_0 \rightarrow 0} \frac{\rho_0}{1 - (1 - \rho_0)^8} = \frac{1}{8}. \quad (6)$$

If we define  $q = 8$  as the neighborhood size, the conditions for an interior equilibrium in the mean-field are, thus,  $\alpha_0 > 1/q$  and  $\alpha_2 > 0$  (fig. 4B).

We can improve the correspondence between the MF and the MDM simulations by noting that the MF includes space implicitly through  $P_{(n_0 \geq 0)}$ , approximated as  $1 - (1 - \rho_0)^8$ . This approximation does not fit simulation results (fig. 7B), but it is possible to obtain a corrected approximation by replacing the MF exponent  $q = 8$  with the exponent  $q'$  fitted to simulation results as a nonlinear least squares estimate. Thus,  $q'$  is obtained from simulation results by fitting  $1 - (1 - \rho_0)^{q'}$  to the relationship between disturbed cell cover  $\rho_0$  and the proportion  $q_{0/2}$  of occupied cells having at least one disturbed neighbor (fig. 7B). This technique was used to approximate the first moment of spatially explicit predator-prey models (Pascual et al. 2000). From the simulation, we obtain  $q' = 3.829$  (fig. 7B). The corrected MF now has  $\alpha_0^* = 1/q' = 0.2612$  as a condition for coexistence, which is closer to  $\alpha_0^* = 0.3$ , obtained in the MDM (fig. 4A; table 1). We used  $q'$  to approximate nearest-neighbor (i.e., between-pair) correlations in the simulation. Although this technique allows us to approximate  $\alpha_0^*$ , it still does not provide a good approximation of mean mussel cover across the parameter space and suggests that higher-order interactions involving units larger than pairs dominate the dynamics.

## Discussion

### The Importance of Local Interactions

The study of environmental complexity often starts from the assumption that physical disturbance imposes spatial structure on communities. This view has been challenged by theoretical and experimental efforts that show that local interactions between physical complexity and biotic processes can lead to nonintuitive large-scale patterns (Roughgarden 1974). Our model suggests that the interaction between global and local processes can be explained without making assumptions about the spatial structure of physical disturbance. Many theoretical studies of disturbance dynamics have further assumed that physical disturbance is a large-scale process that occurs at a much faster temporal scale than do biotic recovery processes (but see Wilson et al. 1996). We demonstrate that the large-scale properties of physical disturbance can result from local interactions and that the separation of temporal scale between disturbance and recovery is not a sufficient reason to ignore local interactions.

When modeling local interactions, we need to test their

**Table 2:** Mussel cover data and scaling exponents at three intertidal mussel beds along the Oregon coast

	Mussel cover				$\beta$	$\gamma$	$\mu$
	1996	1997	1998	1999			
Boiler Bay	.78	.68	.57	.45	1.56	.91	.59
Fogarty Creek	.85	.93	.68	.50	1.54	.91	.58
Yachats North		.89	.84	.87	...	...	...

Note: Scaling exponents are the exponent of cluster size distribution ( $\beta$ ), of perimeter to area ratio ( $\gamma$ ), and of radius of gyration ( $\mu$ ).

validity in natural systems, their ability to explain macroscopic properties of communities, as well as the response of communities to environmental forcing. Local interactions in mussel beds have been suggested as an important factor for recruitment (Petersen 1984) and predation. Those studies have shown the differential strength of mussel attachment as a function of individual size, age, and position (Bell and Gosline 1997; Hunt and Scheibling 2001). The rationale for uncoupling wave disturbance from biotic interactions comes from the assumption that wave disturbance should influence communities at a larger spatial scale and at a much faster rate than do biotic interactions that lead to recolonization. First, our results show that disturbances are highly connected, which challenges the assumption that the spatial structure of wave disturbance is independent from local spreading processes. Second, our model shows that local interactions between disturbance and recovery have nontrivial consequences for mussel bed dynamics even if temporal scales of disturbance and recovery are separate. This is revealed by the persistence of scale-invariant cluster size distribution even when disturbance and recovery rates are very different. Actually, the separation of temporal scales has been shown to be the sufficient condition for SOC in disturbance models that are based on local interactions (Rhodes et al. 1997; Clar et al. 1999).

Many physical variables, including wave force, have a spatial structure at the large scale. This spatial correlation in physical stress has been shown to be responsible for biological patterns in many systems. Our model suggests that abiotic disturbance with no macroscopic structure can generate long-range correlation in communities and that the influence of environmental complexity is not independent of local biotic interactions and does not simply modulate biotic processes. Our results were also robust to the presence of external disturbances with variable size as long as spreading processes are dominant, which was supported by field data.

#### *Percolation Theory and the Extremum Principle*

Scale invariance has been observed for gap distribution in tropical forests (Kubo et al. 1996). Theoretical studies have

also suggested mechanisms that lead to scale invariance in simple predator-prey models (Pascual et al. 2002) and in terrestrial ecosystems (Kizaki and Katori 1999; Hubbell 2001). However, scale invariance associated with phase transitions usually requires fine-tuning of model parameters (Binney et al. 1992) and has been shown in mussel disturbance models in which the disturbance is not an explicit state (Wilson et al. 1996). We still need to understand how communities can self-organize in this critical state under variable environmental conditions. Forest fire models with global tree growth showed that adding an explicit (spreading) disturbance state to lattice models allows us to observe scale invariance without having to fine-tune parameter values, given that disturbance propagation is much faster than growth, which should, in turn, be much faster than external disturbances (i.e., double separation of temporal scales). Our results show that with both growth and disturbance being explicit and local, scale invariance depends only on one separation of temporal scales, namely that disturbance propagation be much faster than external disturbances. This was suggested for other ecological systems with similar antagonistic interactions (Pascual et al. 2002). When imposing a double separation of temporal scales on antagonistic local interactions, Socolar et al. (2001) showed that an additional nonlocal mortality is required in order to observe criticality. The mortality rate at which criticality is observed has also been shown to be an evolutionary stable strategy (Socolar et al. 2001). Our results suggest that self-organized criticality is observed without a slow evolutionary process if the temporal scales of local disturbance and growth are not separate.

We now need to explain the dynamical properties that constrain our model in a critical state. We showed that where scale invariance is observed, mussel cover is close to the percolation threshold. This threshold simply defines the cover at which it becomes possible to cross the lattice by walking on a single “infinite” mussel cluster. Interestingly, this threshold is not influenced by the correlation structure of occupied sites, and the spatially correlated colonization process percolates at the same value as does random colonization, as observed for forest gap models (Kubo et al. 1996). Percolation theory can explain why a system reaches criticality, but it does not provide a complete framework to explain how the system self-organizes itself to this state as parameters are varied. Parameter values that allow the disturbance to persist result in mean mussel cover being maintained close to the percolation threshold. When gaps are able to spread, mussel beds cannot grow to form an infinite cluster because disturbance would then be able to percolate through the lattice. The mean mussel cover within the clustering phase is constrained by the ability of disturbance to percolate through

the contiguous bed. Thus, mussel cover is limited to its minimum value, just below the site percolation threshold. This process has been referred to as the extremum principle and has been used to explain SOC in FFM (Drossel and Schwabl 1992). Since the percolation threshold defines mussel cover at criticality and depends on the neighborhood size, it could provide an additional tool to characterize local spreading in ecological systems from large-scale cover data.

#### Signatures of Oceanographic Regimes

High levels of variability in populations and communities along apparently smooth and mild environmental gradients are widely observed and are explained by unmeasured environmental complexity or by spatial interactions among populations (metapopulation dynamics). We show that threshold phenomena that lead to phase transitions and criticality can explain sharp changes in uncoupled and open populations along continuous gradients of recovery and disturbance rates. By defining all the properties of mussel bed dynamics at the local level, we can predict large-scale properties that are characteristic of the oceanographic forcing (recovery and disturbance). Using a similar model calibrated at one study site, Wootton (2001) accurately predicted observed mussel cover (0.65–0.7) and patterns with a characteristic scale, both compatible with the noncritical region of the  $\alpha_0$  and  $\alpha_2$  parameter space in our model.

Experimental studies have explained the structure of benthic communities as a consequence of local biotic interactions and large-scale oceanographic variability (Menge and Sutherland 1976; Dayton et al. 1992; Menge 1995). While this dual explanation of community structure is linked to the problem of species interactions (top-down effects, competition) versus bottom-up (large-scale oceanographic forcing) control of intertidal communities (Menge 1992, 2000), our model illustrates the causal symmetry between large-scale and local processes (Auyang 1998). More precisely, macroscopic properties of mussel benches emerge from local biotic and abiotic processes and can be predicted only from the knowledge of scaling-up mechanisms. The local interactions are themselves constrained by these emerging properties and by oceanographic forcing that occurs at a much larger scale. This first suggests that the distinction between biotic and abiotic processes should not be used as an indicator of the spatial scales at which these processes occur since local interactions involving physical disturbance generate long-range correlation in spatial patterns. It also means that it is not sufficient to understand how large-scale bottom-up factors such as food/larval concentration and flow regime control small-scale biotic interactions (Nielsen 2001). We must

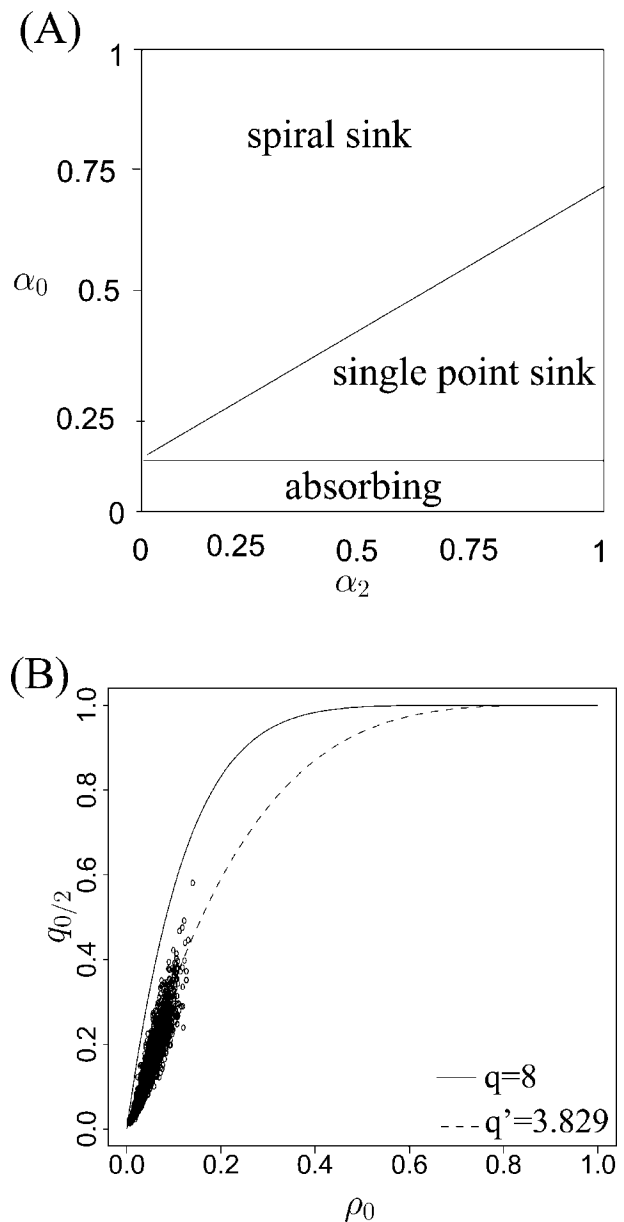


**Figure 7:** A, Parameter space for the mean-field model showing stability regimes (solid lines) as a function of disturbance ( $\alpha_0$ ) and recovery ( $\alpha_2$ ) rates. B, Simulation results for the relationship between proportion of occupied cells having at least one disturbed neighbor ( $q_{0/2}$ ) as a function of disturbed cell cover ( $\rho_0$ ). Lines show the relationship for the fitted exponent  $q'$  (dashed line) and for  $q = 8$  (solid line). Using the *R* statistical package,  $q'$  was obtained as a nonlinear least squares estimate. Simulation results were obtained using  $\alpha_0 = 1$  and  $\alpha_2 = 0.5$ .

also determine how these processes interact spatially and scale-up to generate community structure and dynamics at the site level. Our model provides a simple framework to address this “bottom-up effects on top-down control” across scales (Menge et al. 1997a).

Our results also have important consequences for the management of coastal habitats. We first showed how disturbance dynamics can lead to self-organized patterns and to long-range correlation in benthic communities. Oceanographic conditions that allow self-organization can be defined using critical values and simply require that mussels can colonize the habitat and that disturbances can expand across mussel beds. Under these oceanographic conditions and because of emerging large-scale correlations, local human impacts could affect regional properties and dynamics of coastal systems at scales limited only by habitat fragmentation. Although not all oceanographic regimes should lead to scale invariance, we also showed that mussel abundance can change dramatically as oceanographic conditions change progressively across critical values. Moreover, these critical oceanographic conditions at which changes in mussel cover are observed further depend on their direction (hysteresis; fig. 5). This suggests that community structure should not be expected to return to its initial state following temporary global changes across critical values, such as El Niño–La Niña oscillations or habitat restoration.

#### Acknowledgments

We wish to thank S. Levin for his comments on an earlier version of the manuscript. We also thank M. Pascual and M. Roy for very useful discussions during the development of the model. This is contribution 98 of the Partnership for Interdisciplinary Studies of Coastal Oceans: A Long-Term Ecological Consortium funded by the David and Lucile Packard Foundation. This study was also supported by the Andrew W. Mellon Foundation. F.G. is pleased to acknowledge support from Fonds pour la Formation de Chercheurs et l'Aide à la Recherche.

#### Literature Cited

- Auyang, S. Y. 1998. Foundations of complex-system theories. Cambridge University Press, Cambridge.
- Bascompte, J., and R. Solé. 1995. Rethinking complexity: modelling spatiotemporal dynamics in ecology. *Trends in Ecology & Evolution* 10:361–366.
- Bayne, B. L. 1964. Primary and secondary settlement in *Mytilus edulis* L. (Mollusca). *Journal of Animal Ecology* 33:513–523.
- Bell, E. C., and J. M. Gosline. 1997. Strategies for life in flow: tenacity, morphometry, and probability of dislodgment of two *Mytilus* species. *Marine Ecology Progress Series* 159:197–208.
- Binney, J. J., N. J. Dowrick, A. J. Fisher, and M. E. J. Newman. 1992. The theory of critical phenomena: an introduction to the renormalization group. Clarendon, Oxford.
- Clar, S., B. Drossel, K. Schenk, and F. Schwabl. 1999. Self-organized criticality in forest-fire models. *Physica A* 266: 153–159.
- Day, J. R., and H. P. Possingham. 1995. A stochastic meta-population model with variability in patch size and position. *Theoretical Population Biology* 48:333–360.
- Dayton, P. K., and M. J. Tegner. 1984. Catastrophic storms, El Niño, and patch stability in a southern California kelp community. *Science (Washington, D.C.)* 224: 283–285.
- Dayton, P. K., V. Currie, T. Gerrodette, B. D. Keller, R. Rosenthal, and D. Ven Tresca. 1984. Patch dynamics and stability of some California kelp communities. *Ecological Monographs* 54:253–289.
- Dayton, P. K., M. J. Tegner, P. E. Parnell, and P. B. Edwards. 1992. Temporal and spatial patterns of disturbance and recovery in a kelp forest community. *Ecological Monographs* 62:421–445.
- Denny, M. W. 1987. Lift as a mechanism of patch initiation in mussel beds. *Journal of Experimental Marine Biology and Ecology* 113:231–245.
- Drossel, B., and F. Schwabl. 1992. Self-organized critical forest-fire model. *Physical Review Letters* 69:1629–1632.
- Durrett, R., and S. A. Levin. 1994. Stochastic spatial models: a user's guide to ecological applications. *Philosophical Transactions of the Royal Society of London B, Biological Sciences* 343:329–350.
- Helmuth, B. S. T. 1998. Intertidal mussel microclimates: predicting the body temperature of a sessile invertebrate. *Ecological Monographs* 68:51–74.
- Hubbell, S. P. 2001. The unified neutral theory of biodiversity and biogeography. Vol. 32. *Monographs in population biology*. Princeton University Press, Princeton, N.J.
- Hunt, H. L., and R. E. Scheibling. 2001. Predicting wave dislodgment of mussels: variation in attachment strength with body size, habitat, and season. *Marine Ecology Progress Series* 213:157–164.
- Keeling, M. J. 2000. Evolutionary dynamics in spatial host-parasite systems. Pages 271–291 *in* U. Dieckmann, R. Law, and J. A. J. Metz, eds. *The geometry of ecological interactions*. Cambridge Studies in Adaptive Dynamics. Cambridge University Press, Cambridge.
- Kizaki, S., and M. Katori. 1999. Analysis of canopy-gap structures of forests by ising-gibbs states: equilibrium and scaling property of real forests. *Journal of the Physiological Society of Japan* 68:2553–2560.
- Kubo, T., Y. Iwasa, and N. Furumoto. 1996. Forest spatial dynamics with gap expansion: total gap area and gap size distribution. *Journal of Theoretical Biology* 180: 229–246.

- Levin, S. A. 1992. The problem of pattern and scale in ecology. *Ecology* 73:1943–1967.
- Levin, S. A., and R. T. Paine. 1974. Disturbance, patch formation, and community structure. *Proceedings of the National Academy of Sciences of the USA* 71:2744–2747.
- Malamud, B. D., G. Morein, and D. L. Turcotte. 1998. Forest fires: an example of self-organized critical behavior. *Science (Washington, D.C.)* 281:1840–1842.
- Menge, B. A. 1992. Community regulation: under what conditions are bottom-up factors important on rocky shores? *Ecology* 73:755–765.
- . 1995. Joint bottom-up and top-down regulation of rocky intertidal algal beds in South Africa. *Trends in Ecology & Evolution* 10:431–432.
- . 2000. Top-down and bottom-up community regulation in marine rocky intertidal habitats. *Journal of Experimental Marine Biology and Ecology* 250:257–289.
- Menge, B. A., and J. P. Sutherland. 1976. Species diversity gradients: synthesis of the roles of predation, competition, and temporal heterogeneity. *American Naturalist* 110:351–369.
- . 1987. Community regulation: variation in disturbance, competition, and predation in relation to environmental stress and recruitment. *American Naturalist* 130:730–757.
- Menge, B. A., B. Daley, P. Wheeler, E. Dahlhoff, E. Sanford, and P. Strub. 1997a. Benthic-pelagic links and rocky intertidal communities: bottom-up effects on top-down control? *Proceedings of the National Academy of Sciences of the USA* 94:14530–14535.
- Menge, B. A., B. A. Daley, P. A. Wheeler, and P. T. Strub. 1997b. Rocky intertidal oceanography: an association between community structure and nearshore phytoplankton concentration. *Limnology and Oceanography* 42:57–66.
- Milne, B. T. 1998. Motivation and benefits of complex systems approaches in ecology. *Ecosystems* 1:449–456.
- Nielsen, K. J. 2001. Bottom-up and top-down forces in tide pools: test of a food chain model in an intertidal community. *Ecological Monographs* 71:187–217.
- Pacala, S., and S. A. Levin. 1997. Biologically generated spatial pattern and the coexistence of competing species. Pages 204–232 in D. Tilman and P. Kareiva, eds. *Spatial ecology: the role of space in population dynamics and interspecific interactions*. Princeton University Press, Princeton, N.J.
- Paine, R. T. 1966. Food web complexity and species diversity. *American Naturalist* 100:65–75.
- . 1984. Ecological determinism in the competition for space. *Ecology* 65:1339–1348.
- Paine, R., and S. A. Levin. 1981. Intertidal landscapes: disturbance and the dynamics of pattern. *Ecological Monographs* 51:145–178.
- Pascual, M., P. Mazzega, and S. A. Levin. 2000. Oscillatory dynamics and spatial scales in ecological systems: the role of noise and unresolved pattern. *Ecology* 82:2357–2369.
- Pascual, M., M. Roy, F. Guichard, and G. Flierl. 2002. Cluster size distributions: signatures of self-organization in spatial ecologies. *Philosophical Transactions of the Royal Society of London B, Biological Sciences* 357:657–666.
- Petersen, J. H. 1984. Establishment of mussel beds: attachment behavior and distribution of recently settled mussels (*Mytilus californianus*). *Veliger* 27:7–13.
- Possingham, H. P., and J. Roughgarden. 1990. Spatial population dynamics of a marine organism with a complex life cycle. *Ecology* 71:973–985.
- Reise, K. 1991. Mosaic cycles in the marine benthos. Pages 61–82 in H. Remmert, ed. *The mosaic-cycle concept of ecosystems*. Vol. 85. Ecological studies. Springer, Berlin.
- Rhodes, C. J., H. J. Jensen, and R. M. Anderson. 1997. On the critical behavior of simple epidemics. *Proceedings of the Royal Society of London B, Biological Sciences* 264:1639–1646.
- Rohani, P., T. J. Lewis, D. Grunbaum, and G. D. Ruxton. 1997. Spatial self-organization in ecology: pretty patterns or robust reality? *Trends in Ecology & Evolution* 12:70–74.
- Roughgarden, J. 1974. Population dynamics in a spatially varying environment: how population size tracks spatial variation in carrying capacity. *American Naturalist* 108:649–664.
- Socolar, J. E. S., S. Richards, and W. G. Wilson. 2001. Evolution in a spatially structured population subject to rare epidemics. *Physical Review E* 63:0419081–0419088.
- Solé, R. V., and S. C. Manrubia. 1995a. Are rainforests self-organized in a critical state? *Journal of Theoretical Biology* 173:31–40.
- . 1995b. Self-similarity in rain forests: evidence for a critical state. *Physical Review E* 51:6250–6253.
- Solé, R. V., and J. Valls. 1992. Spiral waves, chaos and multiple attractors in lattice models of interacting populations. *Physics Letters A* 166:123–128.
- Solé, R. V., S. C. Manrubia, M. Benton, S. Kauffman, and P. Bak. 1999. Criticality and scaling in evolutionary ecology. *Trends in Ecology & Evolution* 14:156–160.
- Stauffer, D., and A. Aharony. 1992. *Introduction to percolation theory*. Taylor & Francis, London.
- Svane, I., and I. Setyobudiandi. 1996. Diversity of associated fauna in beds of the blue mussel *Mytilus edulis* L.: effects of location, patch size, and position within a patch. *Ophelia* 45:39–53.
- Tainaka, K. 1989. Stationary pattern of vortices or strings

- in biological systems: lattice version of the Lotka-Volterra model. *Physical Review Letters* 63:2688–2691.
- Tilman, D., and P. Kareiva. 1997. Spatial ecology: the role of space in population dynamics and interspecific interactions. Vol. 30. *Monographs in population biology*. Princeton University Press, Princeton, N.J.
- Wilson, W. G., R. M. Nisbet, A. H. Ross, C. Robles, and R. A. Desharnais. 1996. Abrupt population-changes along smooth environmental gradients. *Bulletin of Mathematical Biology* 58:907–922.
- Wootton, J. T. 2001. Local interactions predict large-scale patterns in empirically derived cellular automata. *Nature* 413:841–844.

Associate Editor: Hugh P. Possingham